AAC Accepted Manuscript Posted Online 3 October 2016 Antimicrob. Agents Chemother. doi:10.1128/AAC.01427-16 Copyright © 2016, American Society for Microbiology. All Rights Reserved.

1 Population Pharmacokinetics of Liposomal Amphotericin B in Immunocompromised

- 2 Children
- 3 Running Title: Pharmacokinetics of liposomal amphotericin in children
- 4 Jodi M. Lestner¹, Andreas H. Groll², Ghaith Aljayyoussi³, Nita L. Seibel^{4,5}, Aziza Shad⁶,
- 5 Corina Gonzalez⁷, Lauren V. Wood⁸, Paul F. Jarosinski⁹, Thomas J. Walsh^{4,10-12}, and William
- 6 W. Hope¹
- 7 1 Antimicrobial Pharmacodynamics and Therapeutics, University of Liverpool, UK
- 8 2 Center for Bone Marrow Transplantation and Department of Pediatric
- 9 Hematology/Oncology, University Children's Hospital Münster, Münster, Germany
- 10 3 Liverpool School of Tropical Medicine, UK
- 11 4 Immunocompromised Host Section, Pediatric Oncology Branch, National Cancer Institute,
- 12 Bethesda, MD, USA
- 13 5 Children's National Medical Center and George Washington University School of
- 14 Medicine and Public Health, Washington, DC, USA
- 15 6 Clinical Investigations Branch, Cancer Treatment Evaluation Program, National Cancer
- 16 Institute, Bethesda, MD, USA
- 17 7 Department of Pediatrics, Division of Pediatric Hematology/Oncology, Georgetown
- 18 University Medical Center, Washington, DC, USA
- 19 8 Center for Cancer Research, National Cancer Institute, Bethesda, MD, USA
- 20 9 Pharmacy Department, National Institutes of Health Clinical Center, Bethesda, MD, USA

21	10 Transplantation-Oncology Infectious Disease Program, Weill Cornell Medical Center,
22	NY, USA
23	11 Department of Pediatrics, Weill Cornell Medical Center, NY, USA
24	12 Department of Microbiology, Weill Cornell Medical Center, NY, USA
25	
26	
27	Corresponding Author: Dr Jodi Lestner
28	Antimicrobial Pharmacodynamics and Therapeutics
29	1.09 Sherrington Building
30	Ashton Rd
31	University of Liverpool
32	Liverpool L69 3GE
33	Telephone +44 (0)151 794 5941
34	Email: jlestner@liverpool.ac.uk
35	
36	Conflicts of Interest
37	WWH has acted as consultant, received research support for Merck, Pfizer Inc., Astellas,
38	Gilead Sciences, F2G.

39	TJW receives research grants for experimental and clinical antimicrobial
40	pharmacotherapeutics from Astellas, Novartis, Merck/Cubist, Pfizer, and Theravance. He has
41	served as consultant to Astellas, Merck/Cubist, Contrafect, Novartis, Pfizer, and Methylgene.
42	AHG has received research grants from Gilead and Merck, Sharp & Dohme, and Pfizer; is a
43	consultant to Astellas, Basilea, Gilead, Merck, Sharp & Dohme, and served at the speakers'
44	bureau of Astellas, Basilea, Gilead, Merck, Sharp & Dohme, Pfizer, Schering-Plough and
45	Zeneus/Cephalon.
46	JML, GA, NS, AS, IB, CG, LVW, PFJ none declared.
47	

48 Keywords

49 Liposomal, amphotericin B, children, pediatrics, pharmacokinetics, invasive fungal disease

51 Abstract

Background Liposomal amphotericin B (LAmB) is widely used in the treatment of invasive
fungal disease (IFD) in adults and children. There are relatively limited PK data to inform
optimal dosing in children that achieves systemic drug exposures comparable to those of
adults.

56 Objectives To describe the pharmacokinetics of LAmB in children aged 1-17 years with
57 suspected or documented IFD.

58 **Methods** Thirty-five children were treated with LAmB at dosages of $2.5-10 \text{ mg kg}^{-1}$ daily.

59 Samples were taken at baseline and at 0.5-2.0 hourly intervals for twenty-four hours after

60 receipt of the first dose (n=35 patients) and on the final day of therapy (n=25 patients).

61 LAmB was measured using high performance liquid chromatography (HPLC). The

62 relationship between drug exposure and development of toxicity was explored.

63 **Results** An evolution in PK was observed during the course of therapy resulting in a 64 proportion of patients (n=13) having significantly higher maximum serum concentration (C_{max}) and area under the concentration time curve (AUC₀₋₂₄) later in the course of therapy, 65 without evidence of drug accumulation (Cmin accumulation ratio, AR < 1.2). The fit of a 2-66 compartment model incorporating weight and an exponential decay function describing 67 68 volume of distribution best described the data. There was a statistically significant relationship between mean AUC₀₋₂₄ and probability of nephrotoxicity (OR 2.37; 95% CI 69 1.84-3.22, p=0.004). 70

Conclusions LAmB exhibits nonlinear pharmacokinetics. A third of children appear to
experience a time-dependent change in PK, which is not explained by weight, maturation or
observed clinical factors.

74 Introduction

75	The small unilamellar liposomal formulation of amphotericin B (LAmB;				
76	AmBisome®) is widely used for the treatment of invasive fungal disease (IFD) in adults and				
77	children. This compound has been available for over two decades and is a first line agent in				
78	the treatment of serious opportunistic diseases that include invasive aspergillosis, invasive				
79	candidiasis, cryptococcal meningoencephalitis, and mucormycosis. (1-4)				
80	Despite extensive clinical experience, many of the details relating to the underlying				
81	pharmacological properties of LAmB remain unclear. A limited number of datasets and				
82	population pharmacokinetic (PK) models have been reported for LAmB. (5-7) These analyses				
83	were based on data gathered from patients receiving relatively low dosages and exclusively				
84	sampled early in the course of therapy. There are very limited data reporting the PK of				
85	LAmB in pediatric populations.				
86	A better understanding of the pharmacological properties of LAmB remains a priority				
87	and would enable optimal dosing, particularly for special populations such as infants and				
88	children. Dosages ranging from 2.5-10 mg kg ⁻¹ per day were studied and each patient was				
89	intensively sampled. The individual PK profiles for a sub-population of participants (n=25)				
90	were compared at the commencement and end of therapy.				

91

Antimicrobial Agents and Chemotherapy

Accepted Manuscript Posted Online

92 Materials & Methods

93 Patients, Antifungal Regimen

This study was designed as a prospective, multi-center, open-label phase II clinical 94 trial. Study protocol approval was obtained from the Ethics Committees of the National 95 Cancer Institute (Bethesda MD, USA); Children's National Medical Center (Washington DC, 96 USA) and Georgetown University Medical Center (Washington DC, USA). Informed consent 97 98 was obtained prior to enrolment in each case. A total of 35 children with a diagnosis of confirmed or suspected IFD were enrolled. Patients received LAmB infused over one hour at 99 dosages of 2.5, 5.0, 7.5, or 10.0 mg kg⁻¹ daily (n= 9, 13, 8, and 8, respectively). Two patients 100 received LAmB as treatment for more than one discrete clinical episode requiring antifungal 101 therapy. Patients undergoing multiple discrete episodes were assigned the same identification 102 number on each occasion and were handled using the dosing reset function in Pmetrics. 103

LAmB (AmBisome®; Gilead Sciences, Inc., Foster City, California) was supplied as
a lyophilized powder and stored at 2-8°C until use. Powder (50 mg) was reconstituted with
12.5 mL of sterile water to a concentration of 4 mg⁻¹ mL, and then further diluted in 5%

107 dextrose. Reconstituted drug was used within 6 hours.

108 Pharmacokinetic Sampling

PK samples were obtained on the first and last day of therapy. The first day of LAmB administration was defined as day one. Heparinized whole-blood samples (0.6-1 mL) were collected by peripheral intravenous catheter. Samples were obtained prior to administration, and at 0.5-2.0 hourly intervals for 24 hours following the start of each infusion. A total of 7-12 samples were obtained per patient within each sampling period (total sampling blood volumes < 3 mL/kg within 24 hours). Sampling was repeated in sixteen patients on the last

Antimicrobial Agents and Chemotherapy

115	day of therapy (12-41 days) using the same sampling schedule. Plasma fractions were
116	separated by centrifugation at 1,500 g for 10 min at 4°C and stored at -80°C until analysis.
117	Concentrations of LAmB in plasma were determined by a high-performance liquid
118	chromatographic assay. (8) Briefly, total active drug and internal standard, 3-nitrophenol,
119	were extracted in methanol and separated by reversed-phase chromatography. The separation
120	was performed isocratically using a Supelcosil ABZ+Plus analytical column (3 μ m particle
121	size, 150 mm x 4.6 mm internal diameter; Supelco, Bellefonte, Pennsylvania), coupled by a
122	Keysone C18 guard column (3 μ m particle size, 7.5 mm x 4.6 mm 7.5 by 4.6 mm; Western
123	Analytical, Murrieta, California). The mobile phase, consisting of 10 mM sodium acetate
124	buffer, including 10 mM EDTA (pH 3.6) and acetonitrile (650:350, vol/vol), was delivered at
125	a flow rate of 1.0 ml/min using a Spectra-Physics Model 250 pump (Thermo Separations, San
126	Jose, California). UV absorbency peaks were detected at a wavelength of 406 nm using a
127	Waters Model 440 UV-VIS detector (Waters Corp, Milford, Massachusetts). Two
128	overlapping standard curves were used: 0.05 to 20 $\mu\text{g/ml}$ and 0.5 to 200 $\mu\text{g/ml}.$ The assay was
129	linear over a range of 0.05-20 and 0.5 to 200 μ g/mL ($r^2 > 0.995$). Intra- and inter-day
130	coefficients of variation were 9.5 and 7.0%, and 5.4 and 6.0%, respectively, and the limit of
131	quantification was 0.05 $\mu\text{g/ml}.$ The average recovery was 90.5% at the concentrations of
132	quality control samples with a standard deviation of 6.2%.

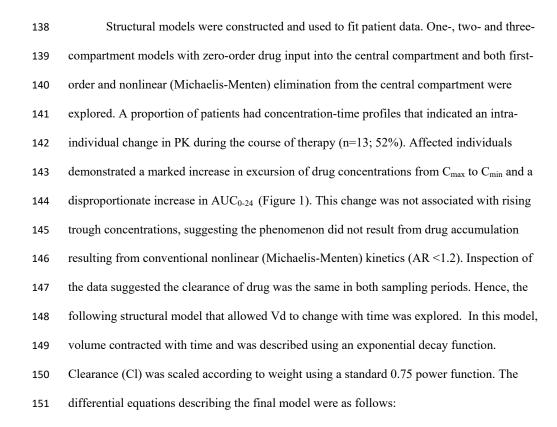
Population Pharmacokinetic Modeling 134

135 Data were analysed using a non-parametric methodology within the program Pmetrics (version 1.2.6; University of Southern California, Los Angeles, CA). (9) The observed data 136

were weighted using the inverse of the estimated assay variance. 137

Antimicrobial Agents and

Chemotherapy



$$\frac{\delta X(1)}{\delta t} = R(1) - (Cl * (\frac{wt}{70})^{0.75}/Vd) * X(1) - Kcp * X(1) + Kpc * X(2)$$
$$\frac{\delta X(2)}{\delta t} = Kcp * X(1) - Kpc * X(2)$$
$$\frac{\delta Vd}{\delta t} = -Vin * K + Vfin$$

152

Where: X(1) and X(2) represent the total (bound and free) amount of LAmB (mg) in the 153 central (c) and peripheral (p) compartments, respectively. R(1), Kcp and Kpc represent the 154 rate of infusion into the central compartment (mg h⁻¹) and first-order inter-compartmental rate 155 156 constants, respectively. Clearance (Cl) is normalised according to a 70 kg individual and 157 allometrically scaled. The volume of the central compartment (Vc) is described by an

exponential decay function in which initial volume (Vin) reduced over time according to arate constant (K) to a final volume (Vfin).

160 The goodness-of-fit of each model to the data was assessed by visual inspection of the 161 observed-predicted values and following linear regression of the observed-predicted values 162 both before after the Bayesian step. The coefficient of determination (r^2) , slope and intercept 163 of each regression were calculated. Statistical comparison of models was based on likelihood 164 ratio, in which twice the likelihood difference was evaluated against a χ^2 distribution with an 165 appropriate number of degrees of freedom. In addition, predictive performance was assessed 166 according to weighted-mean error (a measure of bias) and bias-adjusted weighted-mean-

167 squared error (a measure of precision).

168 The final selected model was validated using a nonparametric bootstrap resampling

169 technique. Three hundred bootstrap datasets were constructed based on random sampling

170 with replacement using ADAPT 5. Measures of central tendency and dispersion and the 95%

171 confidence interval (CI) for each parameter value were calculated and compared with

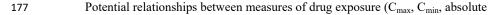
172 estimates from original data. The selected structural model was then implemented within the

173 simulation module of ADAPT 5. (10) Bayesian estimates of the PK parameters for each

174 patient were used to calculate simulated peak plasma concentration (C_{max}), trough plasma

175 concentration (C_{min}), and area under the concentration time curve over 24 hours (AUC₀₋₂₄) at

176 defined therapeutic time points.



178 LAmB dosage, weight adjusted dosage, AUC_{0-24} and mean AUC_{0-24}) and toxicity were

179 explored. Toxicity was defined as changes from baseline values at commencement of therapy

- 180 as follows: nephrotoxicity as an increase in serum creatinine (SCr) of ≥ 0.5 mg/dL or
- 181 doubling of baseline value, hypokalemia as a fall in potassium of $\leq 3.0 \text{ mmol/L}$ or $\geq 50\%$ from

AAC

187

182

183

184

185

186

Results 188

patient during the treatment course.

189	The patient demographics of the study cohort are summarized in table 1. The mean \pm
190	SD weight was 26.9 ± 14.0 kg with a range of 8.8-67.5 kg. There was wide variability in the
191	duration of the rapy: the mean \pm SD was 11.9 \pm 9.41 days of the rapy with a range of 1-41
192	days. The most common underlying diagnosis was hematological malignancy (n =21). Nine
193	patients had undergone allogeneic hematopoietic stem-cell transplantation (HSCT) and 23
194	received concomitant antineoplastic chemotherapy. The majority of patients received LAmB
195	as empirical therapy for suspected IFI (n=31). Seven patients received treatment for
196	confirmed IFI. There were two cases of invasive aspergillosis due to A. fumigatus, and a
197	further case that developed during treatment with LAmB that was classified as a
198	breakthrough infection. Three patients had invasive candidiasis: one central-line infection
199	and one severe oesophagitis due to C. albicans, and one case of candidaemia caused by C.
200	parapsilosis. There was a single case of cryptococcal meningoencephalitis complicating HIV
201	infection. Clinical success was defined according to clinical, radiological, and mycological
202	response during the study period plus relapse-free survival at 2 months after the end of
203	therapy. Clinical success was reported in 76% of probable (n=29) and 43% (n=3) of proven
204	fungal infections.

baseline, anemia as an hemoglobin of ≤8.0 g/dL, and hepatotoxicity as a rise in bilirubin by

 \geq 1.5 mg/dL or AST or ALT \geq 3 times above baseline. A conservative definition was used to

define change in biological parameters in order to overcome variability in sampling between

patients; pre-treatment value was subtracted from the highest measurement observed for each

206	for each patient were plotted against weight. A relationship between the log_{10} -transformed
207	estimates was apparent. The performance of models incorporating an allometric power
208	function was therefore investigated using a scaling exponent fixed at 0.75. No significant
209	relationship was found between Bayesian estimates for volume (Vd) and weight. Differences
210	in clinical factors that might be predicted to alter the PK of LAmB were explored. No
211	significant differences were identified in liver function, serum albumin, white blood cell
212	(WBC) count and total protein concentrations, use of parenteral nutrition and concomitant
213	steroids. A relatively poor fit of standard model structures was apparent (see, for example
214	performance of a standard two-compartment model, figure 2). Conventional compartmental
215	model structures failed to account for the widening excursion of drug concentrations
216	observed in a portion of patients. The parameter estimates for the base and final model are
217	summarized in table 2. The fit of the selected model incorporating a function describing
218	contraction in Vd was satisfactory ($r^2 = 0.90$), and compared favourably to a standard 2-
219	compartment model. The final model consisted of eight support points. Measures of bias and
220	precision were acceptable (see figure 2). The bootstrap mean and 95% CI values for
221	parameters closely approximated the estimates obtained from the final model (table 3),
222	indicating that the parameter estimates from the final model were robust. Both the mean and
223	median parameter values resulted in comparable intercept, slopes and overall r^2 values. The
224	log-likelihood value for the final model was significantly better (more positive) than for the
225	standard 2-compartment model ($\chi^2 = 48.95$, p = <0.001). Figure 3 shows the simulated
226	concentration-time profiles and raw data for two examples of patients that exhibited time-
227	dependent and time-independent changes in PK profiles.
220	Dass announce relationshing mans fouther announced Na completion between the betw
228	Dose-exposure relationships were further explored. No correlation between absolute
229	dose and exposure (C_{max} , C_{min} or AUC ₀₋₂₄) was observed, an expected finding given the

The Bayesian estimates for clearance (Cl) obtained from standard two-compartment models

between dose per-unit-weight and exposure were observed. Plots of dose-normalized Cmax 231 and AUC₀₋₂₄ suggest nonlinearity (figure 4), although a dosing threshold associated with a 232 discrete change in exposure was not observed. 233 234 Transient renal impairment and hypokalemia were common, occurring in 46% (n=16) 235 and 23% (n=8) of patients, respectively. A significant correlation between steady state exposure (AUC₀₋₂₄) and change in serum creatinine (Δ SCr) was observed (Figure 5, r=0.594, 236 p=0.015). A statistically significant relationship between mean AUC₀₋₂₄ and probability of 237 developing nephrotoxicity (OR 2.37; 95% CI 1.84-3.22, p=0.004). There was insufficient 238 239 clinical information to explore the impact of other potential determinants of renal impairment 240 (for example disease severity and concomitant nephrotoxic drugs) in this study cohort. No significant correlations were found between LAmB exposure (in terms of absolute dose, 241 weight adjusted dose, AUC₀₋₂₄ or mean AUC₀₋₂₄) and other toxicity including hypokalemia, 242 243 anemia, and hepatotoxicity.

significant variability in weight within the study population. Significant relationships

244

230

245 Discussion

246	Liposomal amphotericin B is used extensively for the treatment of IFD. Dosages of			
247	3-6 mg kg ⁻¹ are approved in the U.S.A and the E.U. in both adults and children. These			
248	dosages are not based on an in-depth knowledge of the pharmacology of the drug, but rather			
249	results from preclinical in vivo studies and clinical trials that have attempted to identify			
250	regimens that appear safe and effective. There continues to be considerable uncertainty			
251	regarding the lowest effective dosage of LAmB that achieves adequate antifungal effect. As			
252	a result, dosages of 1-15 mg kg ⁻¹ have been studied in a range of clinical settings including			

Antimicrobial Agents and

Chemotherapy

empirical therapy, invasive aspergillosis, invasive candidiasis, and cryptococcal

254 meningoencephalitis. (11-14)

Phase I/II clinical studies of LAmB in children and adults have highlighted variable, 255 dose-dependent PK. Children and adults receiving LAmB at conservative daily doses of 1-3 256 mg kg⁻¹ exhibit linear PK that are described by standard two- or three-compartment models 257 with first-order elimination. (6, 7)(5) Limited data suggest nonlinearity at higher dosages. 258 Walsh et al. observed time-dependent nonlinear PK and an apparent paradoxical dose-259 dependent exposure plateau in adults receiving daily dosages of 7.5-15 mg kg⁻¹. (3) The data 260 from paediatric patients in this study similarly suggests that a proportion of patients exhibit 261 time-dependent nonlinear PK. When the concentration-time profiles of patients exhibiting 262 nonlinear PK are examined a significant excursion in Cmin-Cmin is observed, a change not 263 associated with a proportional increase in half-life that would be expected with classical 264 nonlinear (Michaelis-Menten) clearance, but rather appears to reflect a contraction in the 265 volume of distribution during the course of therapy. Whereas the limited data from adults has 266 267 suggested a paradoxical dose-dependent reduction in exposure at doses $>7.5 \text{ mg kg}^{-1}$, in 268 children higher doses appear to be associated with an increased probability of nonlinearity. The reason for this difference is unclear and warrants further study. 269 High-density lipoproteins (HDL) mediated opsonization of lipid formulations of 270 amphotericin B within plasma has been shown to drive uptake into mononuclear phagocytes 271 and deposition within the liver and spleen. (15-18) Hong et al. reported a negative correlation 272 between Bayesian estimates volume of distribution and the fraction of HDL-associated 273 LAmB in 21 children and adolescence receiving LAmB at daily doses of 0.8-6 mg kg⁻¹. We 274 275 hypothesize that variable HDL saturation and/or phagocyte uptake may be the 276 pathophysiological processes driving the inter-individual variability observed in this study. 277 However, many patients in this small clinical cohort exhibited significant fluctuations in

primarily due to underlying hemato-oncological diagnoses, and we were not able to further 279 characterise relationships between specific hematological parameters and volume contraction. 280 Other significant data such as plasma HDL concentrations were not quantified in this study. 281 This is an interesting hypothesis that warrants further study in experimental models and/or as 282 283 part of larger clinical trials. LAmB is generally well tolerated with a significantly improved 284 toxicity profile when compared to conventional amphotericin B deoxycholate. (14) Dosages of LAmB as high as 15 mg kg⁻¹ daily have been reportedly well tolerated in adults. (3) A 285 number of studies including one large RCT have, however, described dose-dependent toxicity 286 with significantly higher rates of renal impairment and hypokalemia at dosages at or above 10 287 mg kg $^{-1}$ daily. (1) In this study, a significant proportion of patients developed transient renal 288 impairment and/or hypokalemia during the course of treatment. In view of the limited data 289 available, significant inter-individual variability and lack of obvious inflection point in this 290 291 relationship further analysis to define exposure thresholds was not possible. The correlation 292 between drug exposure and Δ SCr observed here suggests, however, that clinical vigilance 293 and assiduous monitoring of renal function is required to minimize the probability of toxicity associated with LAmB. 294

hematological parameters such as WBC count over the course of antifungal therapy,

Taken together these data suggest that a significant proportion of pediatric patients 295 receiving LAmB at daily doses $> 5.0 \text{ mg kg}^{-1}$ exhibit nonlinear PK with significantly higher 296 peak concentrations and overall drug exposure. This phenomenon was not predicted by 297 298 clinical covariates quantified in this study. Therapeutic drug monitoring (TDM) is thus likely to be of value in identifying this subpopulation in order to prevent toxicity. Effective 299 300 implementation of TDM would require a more detailed understand of exposure-toxicity relationships and data describing disease severity in children with proven or probably IFD in 301 order to define target exposure thresholds. 302

Downloaded from http://aac.asm.org/ on October 7, 2016 by LIVERPOOL SCH OF TROPICAL MED

AAC

303 Acknowledgements

304 None declared.

305

306 Funding

307 This study received funding from Astellas Pharma US, Inc..

308

309 References

310	1.	Cornely OA, Maertens J, Bresnik M, Ebrahimi R, Ullmann AJ, Bouza E,		
311		Heussel CP, Lortholary O, Rieger C, Boehme A, Aoun M, Horst HA, Thiebaut		
312		A, Ruhnke M, Reichert D, Vianelli N, Krause SW, Olavarria E, Herbrecht R,		
313		AmBiLoad Trial Study G. 2007. Liposomal amphotericin B as initial therapy for		
314		invasive mold infection: a randomized trial comparing a high-loading dose regimen		
315		with standard dosing (AmBiLoad trial). Clinical infectious diseases : an official		
316		publication of the Infectious Diseases Society of America 44:1289-1297.		
317	2.	Ellis M, Spence D, de Pauw B, Meunier F, Marinus A, Collette L, Sylvester R,		
318		Meis J, Boogaerts M, Selleslag D, Krcmery V, von Sinner W, MacDonald P,		
319		Doyen C, Vandercam B. 1998. An EORTC international multicenter randomized		
320		trial (EORTC number 19923) comparing two dosages of liposomal amphotericin B		
321		for treatment of invasive aspergillosis. Clinical infectious diseases : an official		
322		publication of the Infectious Diseases Society of America 27:1406-1412.		
323	3.	Walsh TJ, Goodman JL, Pappas P, Bekersky I, Buell DN, Roden M, Barrett J,		
324		Anaissie EJ. 2001. Safety, tolerance, and pharmacokinetics of high-dose liposomal		
325		amphotericin B (AmBisome) in patients infected with Aspergillus species and other		
326		filamentous fungi: maximum tolerated dose study. Antimicrobial agents and		
327		chemotherapy 45:3487-3496.		

328	4.	Shoham S, Magill SS, Merz WG, Gonzalez C, Seibel N, Buchanan WL, Knudsen
329		TA, Sarkisova TA, Walsh TJ. 2010. Primary treatment of zygomycosis with
330		liposomal amphotericin B: analysis of 28 cases. Medical mycology 48:511-517.
331	5.	Hong Y, Shaw PJ, Nath CE, Yadav SP, Stephen KR, Earl JW, McLachlan AJ.
332		2006. Population pharmacokinetics of liposomal amphotericin B in pediatric patients
333		with malignant diseases. Antimicrobial agents and chemotherapy 50:935-942.
334	6.	Hope WW, Goodwin J, Felton TW, Ellis M, Stevens DA. 2012. Population
335		pharmacokinetics of conventional and intermittent dosing of liposomal amphotericin
336		B in adults: a first critical step for rational design of innovative regimens.
337		Antimicrobial agents and chemotherapy 56:5303-5308.
338	7.	Wurthwein G, Young C, Lanvers-Kaminsky C, Hempel G, Trame MN,
339		Schwerdtfeger R, Ostermann H, Heinz WJ, Cornely OA, Kolve H, Boos J, Silling
340		G, Groll AH. 2012. Population pharmacokinetics of liposomal amphotericin B and
341		caspofungin in allogeneic hematopoietic stem cell recipients. Antimicrobial agents
342		and chemotherapy 56:536-543.
343	8.	Alak A, Moy S, Bekersky I. 1996. A high-performance liquid chromatographic assay
344		for the determination of amphotericin B serum concentrations after the administration
345		of AmBisome, a liposomal amphotericin B formulation. Therapeutic drug monitoring
346		18: 604-609.
347	9.	Neely MN, van Guilder MG, Yamada WM, Schumitzky A, Jelliffe RW. 2012.
348		Accurate detection of outliers and subpopulations with Pmetrics, a nonparametric and
349		parametric pharmacometric modeling and simulation package for R. Therapeutic drug
350		monitoring 34: 467-476.

351	10.	D'Argenio DZ, Schumitzky A, Wang X. 2009. ADAPT 5 user's guide:
352		pharmacokinetic/pharmacodynamic systems analysis software Biomedical
353		Simulations Resource, Los Angeles, CA.
354	11.	Hamill RJ, Sobel JD, El-Sadr W, Johnson PC, Graybill JR, Javaly K, Barker
355		DE. 2010. Comparison of 2 doses of liposomal amphotericin B and conventional
356		amphotericin B deoxycholate for treatment of AIDS-associated acute cryptococcal
357		meningitis: a randomized, double-blind clinical trial of efficacy and safety. Clinical
358		infectious diseases : an official publication of the Infectious Diseases Society of
359		America 51: 225-232.
360	12.	Hope WW, Castagnola E, Groll AH, Roilides E, Akova M, Arendrup MC,
361		Arikan-Akdagli S, Bassetti M, Bille J, Cornely OA, Cuenca-Estrella M, Donnelly
362		JP, Garbino J, Herbrecht R, Jensen HE, Kullberg BJ, Lass-Florl C, Lortholary
363		O, Meersseman W, Petrikkos G, Richardson MD, Verweij PE, Viscoli C,
364		Ullmann AJ, Group EFIS. 2012. ESCMID* guideline for the diagnosis and
365		management of Candida diseases 2012: prevention and management of invasive
366		infections in neonates and children caused by Candida spp. Clinical microbiology and
367		infection : the official publication of the European Society of Clinical Microbiology
368		and Infectious Diseases 18 Suppl 7:38-52.
369	13.	Walsh TJ, Anaissie EJ, Denning DW, Herbrecht R, Kontoyiannis DP, Marr KA,
370		Morrison VA, Segal BH, Steinbach WJ, Stevens DA, van Burik JA, Wingard JR,
371		Patterson TF, Infectious Diseases Society of A. 2008. Treatment of aspergillosis:
372		clinical practice guidelines of the Infectious Diseases Society of America. Clinical
373		infectious diseases : an official publication of the Infectious Diseases Society of
374		America 46: 327-360.

375	14.	Walsh TJ, Finberg RW, Arndt C, Hiemenz J, Schwartz C, Bodensteiner D,			
376		Pappas P, Seibel N, Greenberg RN, Dummer S, Schuster M, Holcenberg JS.			
377		1999. Liposomal amphotericin B for empirical therapy in patients with persistent			
378		fever and neutropenia. National Institute of Allergy and Infectious Diseases Mycoses			
379		Study Group. The New England journal of medicine 340 :764-771.			
380	15.	Wasan KM, Grossie VB, Jr., Lopez-Berestein G. 1994. Concentrations in serum			
381		and distribution in tissue of free and liposomal amphotericin B in rats during			
382		continuous intralipid infusion. Antimicrobial agents and chemotherapy 38:2224-2226.			
383	16.	Wasan KM, Kennedy AL, Cassidy SM, Ramaswamy M, Holtorf L, Chou JW,			
384		Pritchard PH. 1998. Pharmacokinetics, distribution in serum lipoproteins and			
385		tissues, and renal toxicities of amphotericin B and amphotericin B lipid complex in a			
386		hypercholesterolemic rabbit model: single-dose studies. Antimicrobial agents and			
387		chemotherapy 42: 3146-3152.			
388	17.	Wasan KM, Morton RE, Rosenblum MG, Lopez-Berestein G. 1994. Decreased			
389		toxicity of liposomal amphotericin B due to association of amphotericin B with high-			
390		density lipoproteins: role of lipid transfer protein. Journal of pharmaceutical sciences			
391		83: 1006-1010.			
392	18.	Wasan KM, Rosenblum MG, Cheung L, Lopez-Berestein G. 1994. Influence of			
393		lipoproteins on renal cytotoxicity and antifungal activity of amphotericin B.			
394		Antimicrobial agents and chemotherapy 38: 223-227.			
395					

397 Table 1 Patient demographics of cohorts undergoing sampling on day one of therapy and at

398 steady state

	D (
Demographic	Day one (n=35)	Steady state (n=25)		
Age ($\mu \pm$ SD, range; years)	8.7 ± 4.6 (1 - 17)	$10.5 \pm 6.6 (1 - 17)$		
$rige (\mu = 5D, runge, years)$	$0.7 \pm 1.0(1 - 17)$	10.5 ± 0.0 (1 - 17)		
Gender (M:F)	22:13	15:10		
Weight ($\mu \pm SD$, range; kg)	$26.9 \pm 14.0 \; (8.8 \text{ - } 67.5)$	$25.4 \pm 16.2\;(11.2 - 67.5)$		
Duration of the rapy ($\mu\pm$ SD,	11.9 ± 19.4 (1 - 41)	15.5 ± 11.3 (9.5 - 41)		
range; days)				
/				
Underlying diagnosis (no.				
patients)				
partonito)				
Hematopoietic stem cell				
transplant				
Leukemia	6	5		
		-		
Sickle cell disease	1	1		
Aplastic anemia	1	0		
Chemotherapy				
T 1 '	0	-		
Leukemia	8	5		
Lymphoma	7	5		
Lymphoma	1	5		

Solid tumor	7	4
HIV	4	4
Chronic granulomatous	1	1
disease		
Clinical syndrome (no. patients)		
Established infection	6	6
Empiric treatment	29	19
Pathogen		
Candida albicans	2	2
Candida parapsilosis	1	1
Aspergillus fumigatus	3	3
Cryptosporidium	1	1
Clinical response		
Success	29	21
Failure	8	4
Breakthrough	1	0

400

Parameter	Vin (L)	Vfin (L)	Kcp(h ⁻¹)	Kpc(h ⁻¹)	K (h ⁻¹)	Cl (L h ⁻¹ 70 kg ⁻¹)
		Base	model			
Mean	4.543	n/a	0.28	0.888	n/a	0.488
Median	4.095	n/a	0.184	0.254	n/a	0.545
Standard Deviation	3.44	n/a	0.252	0.387	n/a	0.29
Error (CV%)	75.72	n/a	90.025	43.581	n/a	59.426
		Selecte	d model			
Mean	10.654	2.326	0.21	0.057	0.303	0.67
Median	7.998	2.986	0.178	0.033	0.027	0.665
Standard Deviation	1.523	0.978	0.130	0.01	0.094	0.239
Error (CV%)	14.295	42.064	61.905	17.544	31.023	35.672

403 Table 2. The parameter estimates for the final 2-compartment pharmacokinetic model

404

405 CV%, coefficient of variation; Vin, initial volume of distribution; Vfin, final volume of

406 distribution; K, first-order inter-volume rate constant; Kcp/Kpc, first-order inter-

407 compartmental rate constants; Cl, clearance.

408

409

410

411

412

413

Parameter	Bootstrap		Final model		
	Mean estimate	95% CI	Mean estimate	95% CI	
Vin (L)	10.677	10.646 - 10.87	10.654	10.67 - 10.87	
Vfin (L)	2.345	2.181 - 3.023	2.326	2.162 - 3.01	
$Kcp(h^{-1})$	0.311	0.127 - 0.42	0.210	0.108 - 0.388	
Kpc (h ⁻¹)	0.057	0.043 - 0.061	0.057	0.043 - 0.061	
K (h ⁻¹)	0.303	0.21 - 0.355	0.302	0.21 - 0.351	
Cl (L h^{-1} 70 kg ⁻¹)	0.675	0.555 - 0.781	0.670	0.548 - 0.797	

415 Table 3. Bootstrap estimates of the selected pharmacokinetic model

416

417

418

Figure 1. Concentration-time profiles for each patient on day one of therapy (n=35) and at
completion of therapy (n=25). Closed circles are the raw pharmacokinetic data from each
patient.

422

423 Figure 2. Scatter plots showing observed-versus-predicted values for population

424 pharmacokinetic models after the Bayesian step with a standard 2-compartment model (A)

425 and selected model (B). Open circles, dashed lines and solid lines represent individual

AAC

Antimicrobial Agents and Chemotherapy 426 observed-predicted data points, line of identity, and the linear regression of observed-

427 predicted values, respectively.

428

429	Figure 3. Concentration-time profiles for two patients receiving LAmB (10 mg kg ⁻¹). Initial
430	(Vin) and final (Vfin) estimates for volume of distribution (Vd) are shown. Open circles and
431	solid lines represent the raw data and simulated concentration-time profiles for each patient,
432	respectively. Patient A exhibits evolving PK with a contraction in the Vd while patient B
433	exhibits stable Vd.

434

Figure 4 Comparisons of dose-normalised Cmax (A) and AUC₀₋₂₄ (B) at steady state with
respect to dose per unit weight. Solid and dashed lines represent linear regression and 95%
confidence intervals, respectively.

438

439 Figure 5. Relationship between Bayesian estimates of $AUC_{0.24}$ at steady state with respect to

440 change in serum creatinine. Solid and dashed lines represent linear regression and 95%

441 confidence intervals, respectively.

